2023 IEEE/ASME International Conference on Advanced Intelligent Mechatronics (AIM)
June 28-30, 2023. Seattle, Washington, USA

Full Vehicle Experimental Testing of Semi-active Suspension Equipped with Magnetorheological Dampers

Tiancheng Xu
Department of Research and Development
Shenzhen Upward Technology Co., Ltd.
Shenzhen 518000, People's Republic of China
xutiancheng@upwardtech.cn

Huixing Wang
School of Mechanical Engineering
Nanjing University of Science and Technology
Nanjing 210094, People's Republic of China
huixing_wang@163.com

Yancheng Li
School of Civil and Environmental Engineering
University of Technology Sydney
Ultimo, NSW 2007, Australia
yancheng.li@uts.edu.au

DengXin Leng
Engineering College
Ocean University of China
Qingdao, People's Republic of China
lengdingxin@126.com

Hanou Xu
Shenzhen Upward Technology Co., Ltd.
Shenzhen 518000, People's Republic of China
xuhanou@upwardtech.cn

***Abstract*—This paper presents comprehensive experimental exploration on control performance of magnetorheological (MR) suspension system under various road conditions. MR dampers with monotube structure are designed and installed on front and rear vehicle suspensions. The response time of MR damper force is experimentally determined. Meanwhile, a feasible inverse model is constructed to portray the behavior of the MR dampers based on data obtained from experimental testing with random displacement and current as inputs. An output feedback control strategy is proposed to reduce the vertical response of sprung and unsprung mass, as well as the roll and pitch angles. To be practical, the required feedback signals are relative velocity of MR dampers, the vertical velocity at vehicle mass center, and the angular velocity of roll and pitch which are convenient to collect by commercial sensors like displacement sensor and IMU. To verify the feasibility of the system, a passenger vehicle with four MR dampers suspension was tested on various road profiles. The experiment results indicate the better performance of ride comfort and body attitude of vehicle can be achieved by the proposed MR suspension system.**

Keywords—magnetorheological damper, semi-active control algorithm, output feedback, road test, vehicle ride comfort

I. INTRODUCTION

Semi-active control vehicle suspension, as most promising development, has been paid significant attention recently. So far, vehicle suspensions mainly include three types: passive, semi-active, and active suspension. The suspension is expected to be soft or stiff when the design goal is good ride comfort or road-holding, respectively. It is clear that this is a contradiction for passive damper to find a compromise between two objectives since its dampering is basically unchangeable. On the other hand, the active suspension system is able to produce active force according to control algorithms to meet a high control performance for different design goals and road conditions. However, the limitations of the active suspension include high costs, large energy requirement, and compromising reliability. An attractive device to address these conflicts between cost and performance is the semi-active suspension featuring magnetorheological (MR) damper because it could achieve excellent performance without large energy sources [1].

MR damper as one of the most promising intelligent devices in area of vibration control can alter the damping force by the applied current [2-4]. These features enable the implementation of semi-active vehicle suspension system with relatively low power consumption and great vibration mitigation. For such system, accurate modelling of the complex nonlinear behavior is necessity for control system development. In this regard, Spencer et al. [5] developed a phenomenological model which can adequately portray the nonlinear hysteretic behavior of MR dampers. On the other hand, many studies [6,7,8,9] have investigated the inverse model of MR damper to predict the required command signal to reproduce the desired force. To date, a great deal of research are to design and develop MR damper based suspension in vehicle systems [10,11,12]. Ahmadian and Pare have executed a quarter-car experimental to investigate the control performance of MR suspension with classical on-off control strategy and the results indicted the MR suspension have preferable vehicle stability and ride comfort [13]. Tang et al. proposed a Takagi-Sugeno fuzzy control strategy for semi-active MR suspensions and conducted a quarter-car experiment to validate the performance of the suspension system [14]. Seong et al. utilized the quarter-vehicle

This work was supported by Shenzhen Upward Technology Co,. Ltd.

rig to evaluate the vibration control performance of the MR suspension [15].

Although there are a large number of studies on analytical analysis/simulation of MR damper suspensions and quarter-vehicle rig tests, very few studies have reported on road test of vehicle equipped with MR suspension. Zareh et al. [16] designed and manufactured a low-price prototyped MR damper cooperating with a neuro-fuzzy control strategy. The proposed MR suspension system was installed on a light commercial vehicle and was evaluated by vehicle crossing speed bumps. The vibration results at the front right seat position show the effectiveness of the MR dampers. Jamadar et al. [17] also developed a cost-effective MR damper and installed it on a passenger van for testing; To verify the effectiveness of human simulated intelligent control (HSIC) strategy for MR dampers, Yu et al. [18] implemented half-car simulation and road test of HSIC algorithm on B-level road surface, and the results showed that MR suspension based on HSIC can reduce both vertical vibration and pitch motion. Moreover, Yu et al. carried out the road test on a vehicle with MR damper for evaluating various control strategies [19].

In summary, the MR suspension research conducted road test is lacking and the test road surface mentioned above is speed bump or a rough road, which reflects monotonous type of road excitation; Moreover, most of the performance index are vertical vibration, rather than the pitch and roll motion. In this paper, a comprehensive experimental testing of full vehicle with MR suspension is to be presented with evaluative indices such as vertical acceleration, pitch and roll motion. The paper is organized as follows: Section II introduces the manufactured MR damper and the experiment which is used to measure the force response time of MR damper and to construct the inverse model. Section III and IV include the full vehicle dynamics model and the design of output feedback controller. Finally, section V and VI show the setup and the results of the road test.

II. MAGNETORHEOLOGICAL DAMPER

A MR damper is designed, developed, and manufactured for vehicle suspension semi-active control. This MR damper has a monotube structure and operates in flow modes. The MR Fluid flows through the gap between the sleeve and the piston when the piston moves. The viscosity of MR Fluid changes when a current is applied to magnetic coils, leading to the continuous adjustment of damping force. The dimensions of the commercial MR damper are determined according to the geometry of the target passenger vehicles. Fig. 2 (a) and (b) shows the commercial version of the front and rear MR dampers, respectively.

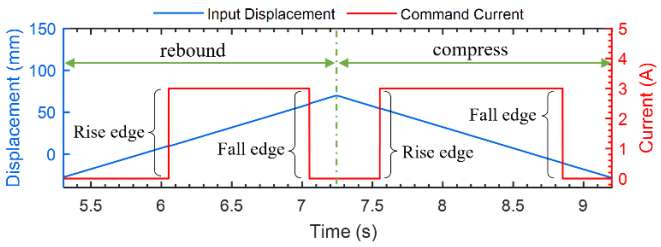

Fig. 1. Illustration of displacement and current inputs in the test.

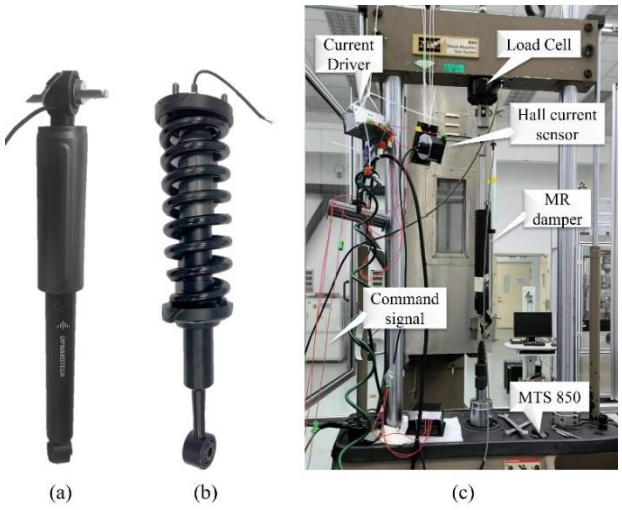

Fig. 2. Photograph of: (a) the commercial front MR damper; (b) the commercial rear MR damper; (c) the experimental setup for response measurement of the Prototyped MR damper.

To explore the dynamic characteristics of the MR damper, a series of experiments are designed for various objectives such as characterization and obtaining response time. The experimental setup is shown in Fig. 2 (c). MTS 850 System is used to drive MR damper according to designed motion. A current driver, e.g., a high current operational amplifier, is adopted to produce an output current for the MR damper according to the command signal. A Hall Effect current sensor is used to feedback drive current applied to MR damper. Besides, SpeedGoat® real-time target machine is used for two purposes: (a) to output command signal to current driver; and (b) to collect the displacement, force, and the current data from MTS built-in sensors and Hall current sensor, respectively.

A. Response Time

The key characteristics to real-time control of MR damper is the ability to change damping force instantaneously. Consequently, one of the critical issues for the application of MR suspension in vibration control is the response time delay of MR damper. It is well-known that the force of magnetorheological fluid (MRF) damper is primarily dependent on the relative velocity and input current. Hence, to measure the transient response (force) of MR damper subjected to current, as shown in Fig. 1, various triangular wave displacements are applied to drive MR damper subjected to various square wave current inputs. The motion of MR damper includes rebound and compress stages. Herein, constant velocities with ± 0.1 m/s, ± 0.2 m/s, and ± 0.3 m/s are selected. In each stage, there is a square wave current with rise and fall edges and the ranges of current are 0-1A, 0-2A, 0-3A in the test.

Here, the current or the force response time of MR damper is considered as the time from the command signal to 90% of the stabilized force response. Furthermore, as shown in Fig. 3, the response times are divided into rise and fall phased with respect to the rise edge and fall edge of the command current, respectively. The force response times for various constant velocities and current ranges are summarized into

TABLE 1. The MR damper can achieve a fast response time of around 10 ms which would be sufficient for real-time control of vehicle dynamics.

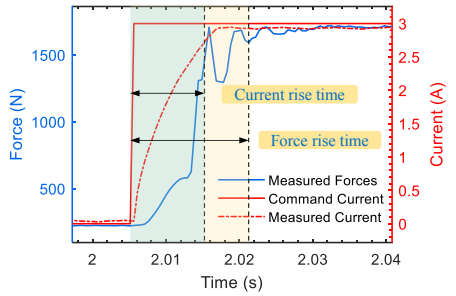

Fig. 3. Illustration of the current and force rise time for rise edge.

TABLE 1. FORCE RESPONSE TIME OF THE MR DAMPER IN VARIOUS COMBINATION OF VELOCITY AND CURRENT

Velocity (m/s)	Current final value (A)	Force response time (ms)			
		Rebound		*Compress*	
		Rise time	*Fall time*	*Rise time*	*Fall time*
0.1	1	7.2	2.9	6.7	1.9
	2	12.8	7.0	9.3	3.2
	3	15.7	8.2	11.7	3.5
0.2	1	6.8	3.0	5.7	1.7
	2	8.3	6.0	8.0	2.5
	3	11.7	6.6	10.5	2.6
0.3	1	9.7	3.1	3.7	0.7
	2	8.1	7.3	8.7	3.8
	3	9.5	5.9	11.8	3.6

B. Inverse Model of Magnetorheological Damper

In this study feedback control is adopted to calculate the control force for the MR dampers. A challenge is how to transform the desired force to an applicable command signal. To address this problem, an inverse model based on polynomial mode for MR damper is developed. For more details, please refer to [8].

III. FULL-CAR MR SUSPENSION MODEL

A mathematical model of a full-car system with four MR dampers is shown in Fig. 4. The vehicle body is regarded as rigid body with three degrees of freedom which are vertical, roll, and pitch directions.

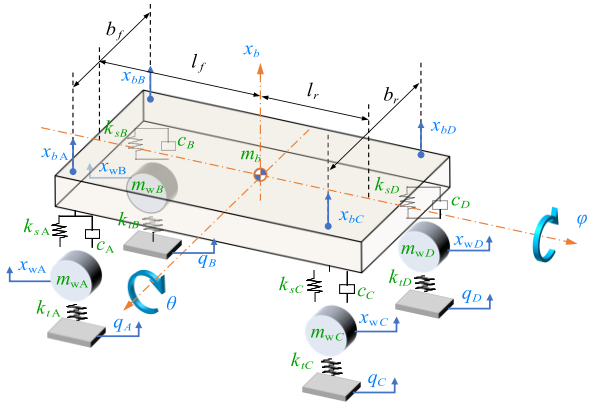

Fig. 4. Schematic of full-car suspension dynamic model

The mass of the vehicle body (sprung mass) is m_b and the rotational inertia of roll and pitch is J_ϕ and J_θ, respectively. The four wheel-axle assembly (unsprung mass) masses, defined by m_{wA}, m_{wB}, m_{wC}, m_{wD}, are assumed to be rigid and each has a degree of freedom in vertical direction. in addition, k_{si}, c_i, and k_{ti} are the equivalent stiffness of suspension, damping of MR dampers, and the equivalent stiffness of tires, respectively, where i=*A, B, C, D* representing four sides of the suspension. The letter x represents the vertical displacement of sprung mass or the tire deflection and the letter q denotes ground excitation. Besides, ϕ and θ are the roll and pitch angles of car body, respectively.

Note that when the roll and pitch angles are small, there have $\sin\phi \approx \phi$ and $\sin\theta \approx \theta$. Based on this, the $(x_{bA},\ x_{bB},\ x_{bC},\ x_{bD})^{\mathrm{T}}$, where the superscript T denotes matrix transpose, can be expressed by $(x_b,\ \phi,\ \theta)^{\mathrm{T}}$ as follows:

$$\begin{aligned} x_{bA} &= x_b + \varphi b_f/2 + l_f\theta \\ x_{bB} &= x_b - \varphi b_f/2 + l_f\theta \\ x_{bC} &= x_b + \varphi b_r/2 - l_r\theta \\ x_{bD} &= x_b - \varphi b_r/2 - l_r\theta \end{aligned} \tag{1}$$

where b_f and b_r are the wheel-center-distances of front and rear wheel, respectively, while l_f and l_r are the distances from the front and rear edge to the center of gravity. Therefore, there are 7 independent DOFs in the system. The governing equations of motion for the 7-DOFs MR suspension system can be derived in matrix form as follows:

$$\begin{cases} \mathbf{M_b}\ddot{\mathbf{X}}_\mathbf{b} = -\mathbf{H}^{\mathrm{T}}\mathbf{K_b}(\mathbf{H}\mathbf{X_b} - \mathbf{X_t}) - \mathbf{H}^{\mathrm{T}}\mathbf{u} \\ \mathbf{M_t}\ddot{\mathbf{X}}_\mathbf{t} = \mathbf{K_b}(\mathbf{H}\mathbf{X_b} - \mathbf{X_t}) - \mathbf{K_t}(\mathbf{X_t} - \mathbf{q}) + \mathbf{u} \end{cases} \tag{2}$$

where the dot on the variable denotes the derivative with respect to time, moreover, the matrixes in (2) are given as follows:

$$\begin{aligned} &\mathbf{X_t} = \begin{pmatrix} x_{wA} \\ x_{wB} \\ x_{wC} \\ x_{wD} \end{pmatrix},\ \mathbf{X_b} = \begin{pmatrix} x_b \\ \varphi \\ \theta \end{pmatrix},\ \mathbf{q} = \begin{pmatrix} q_A \\ q_B \\ q_C \\ q_d \end{pmatrix},\ \mathbf{M_b} = \begin{vmatrix} m_b & & \\ & J_\varphi & \\ & & J_\theta \end{vmatrix}, \\ &\mathbf{K_b} = \begin{vmatrix} k_{sA} & & & \\ & k_{sB} & & \\ & & k_{sC} & \\ & & & k_{sD} \end{vmatrix},\ \mathbf{H} = \begin{bmatrix} 1 & l & l_f \\ 1 & -l & l_f \\ 1 & l & -l_r \\ 1 & -l & -l_r \end{bmatrix}, \\ &\mathbf{M_t} = \begin{vmatrix} m_{wA} & & & \\ & m_{wB} & & \\ & & m_{wC} & \\ & & & m_{wD} \end{vmatrix},\ \mathbf{K_t} = \begin{vmatrix} k_{tA} & & & \\ & k_{tB} & & \\ & & k_{tC} & \\ & & & k_{tD} \end{vmatrix},\ \mathbf{u} = \begin{vmatrix} F_{dA} \\ F_{dB} \\ F_{dC} \\ F_{dD} \end{vmatrix}, \end{aligned} \tag{3}$$

where $u = (F_{dA},\ F_{dB},\ F_{dC},\ F_{dD})^{\mathrm{T}}$ representing the control force vector of MR dampers. Let $\tilde{\mathbf{X}} = [\mathbf{X_b^{\mathrm{T}}}\ \mathbf{X_t^{\mathrm{T}}}]^{\mathrm{T}}$, then the (2) can be rewritten as

$$\mathbf{M}\ddot{\tilde{\mathbf{X}}} + \mathbf{K}\tilde{\mathbf{X}} = \mathbf{E_1}\mathbf{q} + \mathbf{E_2}\mathbf{u} \tag{4}$$

where

$$\mathbf{M}=\begin{vmatrix}\mathbf{M_b} & \\ & \mathbf{M_t}\end{vmatrix},\ \mathbf{K}=\begin{vmatrix}\mathbf{H}^{\mathrm{T}}\mathbf{K_b}\mathbf{H} & -\mathbf{H}^{\mathrm{T}}\mathbf{K_b}\\ -\mathbf{K_b}\mathbf{H} & \mathbf{K_b}+\mathbf{K_t}\end{vmatrix},$$
$$\mathbf{E_1}=\begin{bmatrix}\mathbf{0}\\ \mathbf{K_t}\end{bmatrix},\ \mathbf{E_2}=\begin{bmatrix}-\mathbf{H}^{\mathrm{T}}\\ \mathbf{I}\end{bmatrix} \tag{5}$$

where $\mathbf{I}$ is the unit matrix. Furthermore, let $\mathbf{X}=\begin{bmatrix}\tilde{\mathbf{X}}^{\mathrm{T}} & \dot{\tilde{\mathbf{X}}}^{\mathrm{T}}\end{bmatrix}^{\mathbf{T}}$, then the (4) can be rewritten in form of state space as

$$\begin{cases}\dot{\mathbf{X}}=\mathbf{AX}+\mathbf{BU}\\ \mathbf{Y}=\mathbf{CX}\end{cases} \tag{6}$$

where

$$\mathbf{A}=\begin{vmatrix}\mathbf{0} & \mathbf{I}\\ -\dfrac{\mathbf{K}}{\mathbf{M}} & \mathbf{0}\end{vmatrix},\ \mathbf{B}=\begin{bmatrix}\mathbf{0} & \mathbf{0}\\ \dfrac{\mathbf{E_1}}{\mathbf{M}} & \dfrac{\mathbf{E_2}}{\mathbf{M}}\end{bmatrix},\ \mathbf{U}=\begin{bmatrix}\mathbf{q}\\ \mathbf{u}\end{bmatrix} \tag{7}$$

Note that the output vector $\mathbf{Y}$ and the output matrix $\mathbf{C}$ are undetermined.

IV. Semi-Active Controller Design

For semi-active control systems, the design of the controller is one of the most important parts. A classical and commonly used algorithm is the state feedback control. The main feature is that the internal states of the system need to be fully known and this limits its application in practical engineering. For instance, a 7 DOFs full-vehicle system has 14 state signals:

$$\mathbf{X}=[x_b\ \phi\ \theta\ x_{\mathrm{wA}}\ x_{\mathrm{wB}}\ x_{\mathrm{wC}}\ x_{\mathrm{wD}}\ \dot{x}_b\ \dot{\phi}\ \dot{\theta}\ \dot{x}_{\mathrm{wA}}\ \dot{x}_{\mathrm{wB}}\ \dot{x}_{\mathrm{wC}}\ \dot{x}_{\mathrm{wD}}]^T \tag{8}$$

need to measure and this is often inconvenient and high cost for commercialization, especially the 7 displacement signals are difficult to measure in practical. In most existing studies, all the system states were often assumed as measurable, i.e., a full-state feedback controller was adopted. However, it is clear that the full-state feedback control is impractical. In this study, an output feedback controller, which utilize output $\mathbf{Y}$ as feedback signal to control itself, is proposed to obtain the desired control force which is feasible for engineering application.

A. Output Feedback Controller

First, a LQR should be designed to minimize the output $\mathbf{Y}$ instead of the state $\mathbf{X}$ for following system:

$$\begin{cases}\dot{\mathbf{X}}=\mathbf{AX}+\mathbf{Bu}\\ \mathbf{Y}=\mathbf{CX}\end{cases} \tag{9}$$

If a system is controllable then there is a unique optimal state feedback law $\mathbf{u}=-\mathbf{F_{state}}\mathbf{X}$ to minimize the quadratic cost function $J(\mathbf{u})$ as follows:

$$J(\mathbf{u})=\int_0^{\infty}(\mathbf{Y}^{\mathrm{T}}\mathbf{QY}+\mathbf{u}^{\mathrm{T}}\mathbf{Ru})\ d\mathrm{t} \tag{10}$$

where $\mathbf{Q},\ \mathbf{R}$ are the symmetric weighting matrices.

Nevertheless, the states are frequently impossible or difficult to measure in practical engineering. Based on this, an alternative method is to use output signal $\mathbf{Y}$, which is generally more convenient to measure than state signals $\mathbf{X}$, as feedback signal to calculate the control force, i.e., $\mathbf{u}=-\mathbf{F_{output}}\mathbf{Y}$. The ideal performance of output feedback is as follows:

$$\mathbf{u}=-\mathbf{F_{state}}\mathbf{X}=-\mathbf{F_{output}}\mathbf{Y}=-\mathbf{F_{output}}\mathbf{CX} \tag{11}$$

one can obtain

$$\mathbf{F_{state}}=\mathbf{F_{output}}\mathbf{C} \tag{12}$$

Although the general solution of $\mathbf{F_{output}}$ in (12) is difficult to obtain and may not even exist. The accuracy analysis solution is not necessary for engineering application; thus, a feasible approach is to search a matrix $\mathbf{F_{output}}$ which make the output feedback system has a similar pole location with state feedback system by numerical search procedure. For a given system, we have

$$\min_{\mathbf{F_{output}}}\ J=\|L\|_2=\sqrt{\sum_{i=1}^{14}|p_i^{state}-p_i^{output}|^2}$$
$$\textbf{subject to}:\ \mathrm{Re}[p^{output}]<\mathbf{0}_{1\times 14} \tag{13}$$

where $\mathrm{Re}[\cdot]$ denotes the real part of a complex number; $p^{state}=(p_1^{state},\ p_2^{state},...,\ p_{14}^{state})$ is the eigenvalue vector of $|\mathbf{A}-\mathbf{BF_{state}}|$ and $p^{output}=(p_1^{output},\ p_2^{output},...,\ p_{14}^{output})$ is the eigenvalue vector of $|\mathbf{A}-\mathbf{BF_{output}}|$; The constraint condition are used to ensure that all the pole points of the output feedback system are in the left-half of s plane, i.e., the output feedback system is stabilizable. In addition, the initial value of $\mathbf{F_{output}}$ is calculated as

$$\hat{\mathbf{F}}_{\mathbf{output}}=\mathbf{F_{state}}\cdot pinv[\mathbf{C}] \tag{14}$$

where $pinv[\cdot]$ denotes the Moore-Penrose inverse of a matrix. In fact, sometimes, the performance of an output feedback system with $\hat{\mathbf{F}}_{\mathbf{output}}$ is close enough to that of a state feedback system.

Ultimately, the desired control force F_d, the relative velocity, and the relative displacement of suspension are imported into inverse model to calculate the desired current I_i. Considering the property of the MRD and the hardware configuration, the real control current should meet the following conditions:

$$I=\begin{cases}I_{\mathrm{i}},\ \text{when}\ 0\leqslant I_{\mathrm{i}}\leqslant I_{max}\\ 0,\ \text{when}\ I_{\mathrm{i}}<0\ \text{or}\ |\dot{x}_{sw}|\leqslant 0.03\,\mathrm{m/s}\\ I_{max},\ \text{when}\ I_{\mathrm{i}}>I_{max}\end{cases} \tag{15}$$

B. Signals and Sensors

In the previous sections, an output feedback controller is designed to control system output $\mathbf{Y}$ by measuring $\mathbf{Y}$ itself. Hence the selection of $\mathbf{Y}$ is important in this design. It is readily straightforward to conclude that the $\mathbf{Y}$ should: (a) be easy to measure; (b) directly influence the ride comfort and roadholding; and (c) close to the performance of state feedback. Through the analysis of sensors and trial and error in the simulator, the output matrix $\mathbf{C}$ is chosen as follows:

$$\mathbf{C} = \begin{bmatrix} \mathbf{I}_{3\times 3} & \mathbf{0}_{3\times 4} \\ \mathbf{H} & -\mathbf{I}_{4\times 4} \end{bmatrix} \tag{16}$$

Then the $\mathbf{Y}$ can be written as

$$\begin{aligned} \mathbf{Y} &= \mathbf{CX} \\ &= [\dot{x}_b,\ \dot{\phi},\ \dot{\theta},\ \dot{x}_{sA} - \dot{x}_{\mathrm{wA}}, \dot{x}_{s\mathrm{B}} - \dot{x}_{\mathrm{wB}},\ \dot{x}_{s\mathrm{C}} - \dot{x}_{\mathrm{wC}},\ \dot{x}_{s\mathrm{D}} - \dot{x}_{\mathrm{wD}}]^T \end{aligned} \tag{17}$$

where the $\dot{x}_b,\ \dot{\phi},\ \dot{\theta}$ can expediently be measured by Inertial Measurement Unit (IMU), whereas the $\dot{x}_{sA} - \dot{x}_{\mathrm{wA}}$, $\dot{x}_{s\mathrm{B}} - \dot{x}_{\mathrm{wB}}$, $\dot{x}_{s\mathrm{C}} - \dot{x}_{\mathrm{wC}}$, $\dot{x}_{s\mathrm{D}} - \dot{x}_{\mathrm{wD}}$can be obtained by taking the derivative of the relative displacement measured by displacement sensor and the lowpass filtering. Note that the relative displacement and velocity can also be utilized for inverse model to predict command current. The block diagram of MRD suspension and control system is shown in Fig. 5.

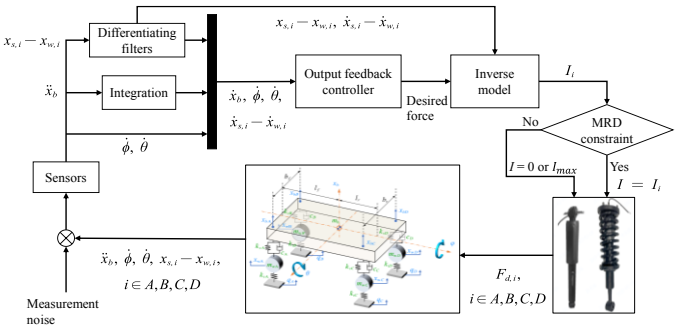

Fig. 5. Block-diagram of the MR dampers suspension with semi-active output feedback control system

V. Experimental Setup

In order to verify the effectiveness of the manufactured MR damper and the proposed output feedback control algorithm in practice, a full vehicle test was carried out on standard roads to evaluate the control performance of the MR suspension system.

The MR suspension system mainly includes four parts: controller, actuator, sensors, and interface. The controller consists of a SpeedGoat® real-time target machine and control algorithm programs. The actuator is composed of four MR dampers and corresponding current amplifiers. An IMU and four displacement sensors are used here to measure vehicle responses. An upper computer is to execute control algorithms, monitor data and so on. The control algorithm, signal processing and inverse model of MR damper were built in MATLAB/Simulink. The Simulink programs are compiled and downloaded into Speedgoat, and the control signals are amplified by the current amplifiers to regulate the MR dampers.

An urban off-road vehicle was selected as the test vehicle. the passive dampers of the original car are replaced by the MR dampers, as shown in the Fig. 6**Error! Reference source not found.** (a) and (b). The two ends of the displacement sensor are fixed on sprung mass and unsprung mass Fig. 6**Error! Reference source not found.** (**Error! Reference source not found.Error! Reference source not found.**b) to measure angular variation, which can be transformed to linear displacement after standardization, between both ends. The IMU, used to measure acceleration, roll, and pitch velocity, needs be placed at center of mass of the vehicle. Therefore, the IMU is mounted at cup holder Fig. 6**Error! Reference source not found.** (**Error! Reference source not found.Error! Reference source not found.**c) according to the practical situation. Besides, the Speedgoat and the current driver are placed at boot as shown in Fig. 6**Error! Reference source not found.Error! Reference source not found.** (d). Considering that the main frequency range of suspension response is between 0-50 Hz, the basic frequency of controller is set as 500 Hz.

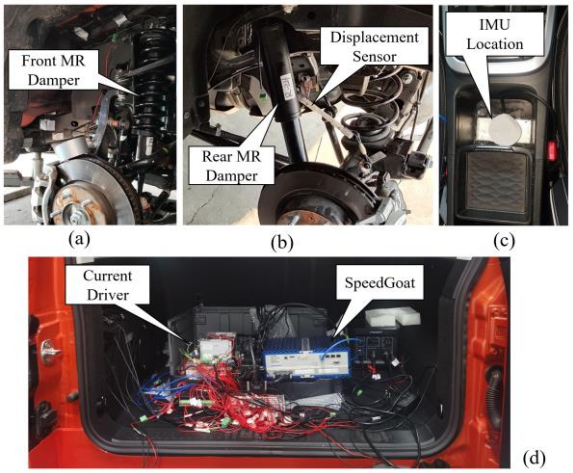

Fig. 6. Photograph of the prototype MR suspension control system: (a) Installation of the front MR damper; (b) Installation of the rear MR damper and the displacement sensor; (c) Installation position of the IMU; (d) Position of the Speedgoat machine and the Current Driver.

VI. Road Test and Results

To comprehensively evaluate the control performance of the MR suspension, the vehicle equipped with prototype MR semi-active suspension system was tested in proving ground. The photographs of three representative roads are shown in Fig. 7. Fig. 7 (a) is the resonance road which the height of step is 13mm and this road could excite the vertical resonance of vehicle. Fig. 7 (b) is the square pit road which the depth of pit is 80mm and mainly lead to pitch or roll motion. Furthermore, Fig. 7 (c) shown the left side of the undulating road. When a vehicle is driving on the undulating road, the vehicle may simultaneously generate pitch and roll motion and even a large vertical acceleration when the wheels are off the ground.

Fig. 7. Photograph of the test road: (a) resonance road; (b) square pit road; (c) undulating road.

The original car with passive dampers and the refitted car which the passive dampers all are replaced by four MR dampers

are requested to pass all the roads at the same speed and load. The passing speed of resonance road, square pit road, and undulating road are 30kph, 10kph, and 70kph, respectively. The responses at vehicle centroid are represented in time and frequency field as below.

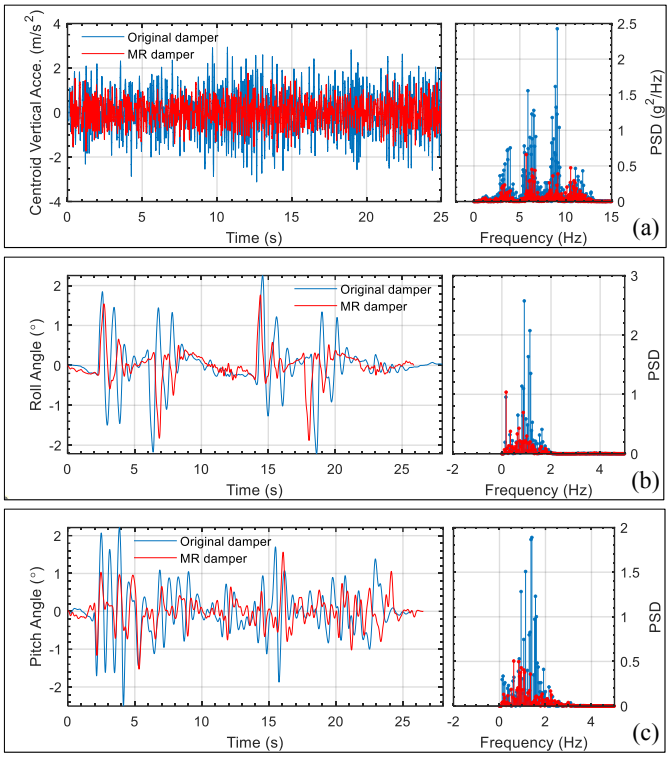

Fig. 8. Time and frequency responses of: (a) centroid vertical acceleration when passing resonance road; (b) roll angel when passing square pit road; (c) pitch angle when passing undulating road.

From Fig. 8, it can be seen that the proposed MR suspension represents superior ride comfort than original passive damper. The percentage reduction of max responses of the MR suspension relative to the passive damper are 42.91%, 16.38%, and 37.60%, and the ones of RMS responses are 42.01%, 32.47%, and 40.98%. Besides, the decline also occurred at all frequency ranges.

VII. Conclusions

In this study, a semi-active MR suspension is proposed based on a commercial MR damper and an output feedback controller. A commercial vehicle equipped with the proposed MR suspension system is tested under various representative roads. The test results indicate that the proposed MR suspension has superior performance for control on vertical acceleration, roll angle, and pitch angle of vehicle body in comparison with original passive suspension.

Acknowledgment

The authors acknowledge Mr Jian Wang for his valuable advisory with the data acquisition & road testing, and Mr Ziming Zhang & Mr Jianlong Zhao for their technical support in the experimental testing of MR damper.

References

[1] Savaresi, Sergio M., Charles Poussot-Vassal, Cristiano Spelta, Olivier Sename, and Luc Dugard. Semi-active suspension control design for vehicles. Elsevier, 2010.

[2] Rabinow J 1948 Magnetic Fluid Clutch *National Bureau of Standards Technical News Bulletin 32* 54-60

[3] Li, Y., Li, J., Li, W. & Du, H. (2014). A state-of-the-art review on magnetorheological elastomer devices. Smart Materials and Structures, 23 (12), 1-24.

[4] Hu, Hongsheng, et al. "Design, modeling, and controlling of a large-scale magnetorheological shock absorber under high impact load." Journal of Intelligent Material Systems and Structures 23.6 (2012): 635-645.

[5] Spencer Jr, B., Dyke, S.J., Sain, M.K. and Carlson, J., 1997. Phenomenological model for magnetorheological dampers. Journal of engineering mechanics, 123(3), pp.230-238.

[6] Xia, P.Q., 2003. An inverse model of MR damper using optimal neural network and system identification. Journal of sound and vibration, 266(5), pp.1009-1023.

[7] Gu, Xiaoyu, Yang Yu, Jianchun Li, and Yancheng Li. "Semi-active control of magnetorheological elastomer base isolation system utilising learning-based inverse model." Journal of Sound and Vibration 406 (2017): 346-362.

[8] Choi, S-B., S-K. Lee, and Y-P. Park. "A hysteresis model for the field-dependent damping force of a magnetorheological damper." Journal of sound and vibration 2, no. 245 (2001): 375-383.

[9] Wang, D. H., and W. H. Liao. "Modeling and control of magnetorheological fluid dampers using neural networks." Smart materials and structures 14, no. 1 (2004): 111.

[10] Choi, Seung-Bok, and Young-Min Han. Magnetorheological fluid technology: applications in vehicle systems. CRC press, 2012.

[11] Choi, Seung-Bok, Hwan-Soo Lee, and Young-Pil Park. "H8 control performance of a full-vehicle suspension featuring magnetorheological dampers." Vehicle System Dynamics 38, no. 5 (2002): 341-360.

[12] Yoon, Dal-Seong, Gi-Woo Kim, and Seung-Bok Choi. "Response time of magnetorheological dampers to current inputs in a semi-active suspension system: Modeling, control and sensitivity analysis." Mechanical Systems and Signal Processing 146 (2021): 106999.

[13] Ahmadian, Mehdi, and Christopher A. Pare. "A quarter-car experimental analysis of alternative semiactive control methods." Journal of Intelligent Material Systems and Structures 11, no. 8 (2000): 604-612.

[14] Tang, Xin, Haiping Du, Shuaishuai Sun, Donghong Ning, Zhiwei Xing, and Weihua Li. "Takagi–Sugeno fuzzy control for semi-active vehicle suspension with a magnetorheological damper and experimental validation." IEEE/ASME transactions on mechatronics 22, no. 1 (2016): 291-300.

[15] Seong, Min-Sang, Seung-Bok Choi, and Young-Min Han. "Damping force control of a vehicle MR damper using a Preisach hysteretic compensator." Smart materials and structures 18, no. 7 (2009): 074008.

[16] Zareh, Seiyed Hamid, Farshad Matbou, and Amir Ali Akbar Khayyat. "Experiment of new laboratory prototyped magneto-rheological dampers on a light commercial vehicle using neuro-fuzzy algorithm." Journal of Vibration and Control 21, no. 15 (2015): 3007-3019.

[17] Jamadar, Mohibb E. Hussain, Pinjala Devikiran, Rangaraj Madhavrao Desai, Hemantha Kumar, and Sharnappa Joladarashi. "Real-time testing and thermal characterization of a cost-effective magneto-rheological (MR) damper for four-wheeler application." Journal of the Brazilian Society of Mechanical Sciences and Engineering 45, no. 2 (2023): 95.

[18] Yu, Miao, X. M. Dong, Seung Bok Choi, and C. R. Liao. "Human simulated intelligent control of vehicle suspension system with MR dampers." Journal of Sound and Vibration 319, no. 3-5 (2009): 753-767.

[19] Yu, Miao, Seung Bok Choi, X. M. Dong, and C. R. Liao. "Fuzzy neural network control for vehicle stability utilizing magnetorheological suspension system." Journal of Intelligent Material Systems and Structures 20, no. 4 (2009): 457-466.